Sensitivity of Ce doped CuO for NO_2 gas

Isam M. Ibrahim[1], Jobair A. Najim[2], Aws M. Rakea[2]

[1]Department of Physics, College Science, University of Baghdad, Iraq

[2]Department of Physics, College Science, University of Anbar, Iraq

E-mail: dr.issamiq@gmail.com

Abstract

In this work the structural, optical and sensitive properties of Cerium - Copper oxide thin film prepared on silicon and glass substrate by the spray pyrolysis technique at a temperature of (200, 250, 300 °C). The results of (XRD) showed that all the prepared films were of a polycrystalline installation and monoclinic crystal structure with a preferable directions was $(11\bar{1})$ of CuO. Optical characteristics observed that the absorption coefficient has values for all the prepared CuO: Ce% (10^4 cm^{-1}) in the visible spectrum, indicating that all the thin films prepared have a direct energy gap. Been fabrication of gas sensors of (CuO: Ce %) within optimum preparation conditions and study sensitivity properties were examined her exposed to nitrogen dioxide (NO_2) with concentration ratio of 3 %, at operating temperatures (R.T, 200 and 300 °C). It is found that the maximum sensitivity at concentration value (Ce=50 %) which it is equal to (39.15 %) at operating temperature (300 °C).

Key words

Optical and sensitive properties, thin film, CuO:CeO.

Article info.

Received: May. 2017
Accepted: Jun. 2017
Published: Dec. 2017

تحسسية أوكسيد النحاس المطعم بالسيريوم لغاز ثاني أوكسيد النتروجين (NO_2)

عصام محمد ابراهيم[1]، جبير عبدالله نجم[2]، أوس موفق راكع[2]

[1]قسم الفيزياء، كلية العلوم، جامعة بغداد، العراق

[2]قسم الفيزياء، كلية العلوم، جامعة الأنبار، العراق

الخلاصة

تم في هذا البحث مناقشة الخصائص التركيبية، البصرية والتحسسية لأغشية أوكسيد السيريوم - أوكسيد النحاس الرقيقة المرسبة على قواعد من السليكون والزجاج بواسطة تقنية التحلل الكيميائي الحراري في درجات حرارة مختلفة (200، 250، 300 ℃) وأظهرت نتائج حيود الاشعة السينية (XRD) أن جميع الاغشية المحضرة تمتلك تركيب متعدد التبلور (polycrystalline) أحادية الميل (monoclinic) وان الاتجاه المفضل هو (111). ولوحظ من الخصائص البصرية ان قيمة معامل الامتصاص لجميع اغشية (CuO:Ce) هي (10^4 cm^{-1}) في منطقة الطيف المرئي وهذا يعني ان جميع الاغشية الرقيقة المحضرة تمتلك فجوة طاقة مباشرة. تم تصنيع خلية متحسس غاز من اغشية (CuO:Ce) ضمن ظروف التحضير المثلى وتم دراسة الخواص التحسسية لها بتعريضها لغاز ثاني اوكسيد النتروجين (NO_2) بنسبة 3 %، و ان افضل درجة حرارة تشغيل للمتحسس هي (300 °C و 200). وجد ان اعظم قيمة للحساسية عند نسبة اضافة (Ce=50%) والتي تساوي (39.15%) عند درجة حرارة (300 °C).

Introduction

The study and application of thin film technology is entirely entered in to almost all the branches of science and technology. Present study which describes the synthesis and study of optical, structural characteristics of cerium doped Copper oxide (CuO) is really more interesting for researchers due to its vast applications [1]. Due to the properties like reflectivity, transparency, low electrical sheet

resistance etc. copper oxide thin films has immense applications such as gas sensor devices [2] Solar application [3, 4], magnetic devices [5], magnetic storage media [6], Optoelectronic Device [7], field emission [8]. Till to day so many methods were adopted to synthesize doped or un-doped copper oxide films such as electro deposition [9], spraying [10], CVD [11], thermal oxidation [12], MBE [13], plasma based ion implantation and deposition [14] and reactive sputtering Laser Pulses Evaporation, spray pyrolysis [15]. Copper oxide crystallizes monoclinic structure with lattice constant (4.27 Å). It is an p-type semiconductor having law band gap energy (≈1.27-1.58 eV) [16, 17] and the wavelength Cutting material (CuOs) is (680) nm, either absorptions coefficient is (10^4 cm^{-1}) when wavelength (500) nm, Since Used in optical thermal complexes which require high efficiency and good range of stability and high absorbency in extent the visible wavelength [16, 18].

Experimental

Ce doped thin films at different concentration (10, 20, 30, 40 and 50 vol. %) of cerium, were prepared by chemical spray pyrolysis. The films deposited on silicon and micro-glass slides were first cleaned with detergent water and then dipped in Alcohol. Spray solution was prepared by mixing 0.1 M aqueous solutions of $CuCl_2$ and $CeCl_4$ at ratio (10, 20, 30, 40 and 50 vol. %) using a magnetic stirrer. The automated spray solution was then transferred to the hot substrate kept at the normalized deposition temperature of (200, 250 and 300 °C) using filtered air as carrier gas at a flow rate normalized to approximately (2.3) ml/min, to prevent the substrate from excessively cooling. The structural properties were determined by X-ray diffraction (XRD- 6000 Labx, supplied by Shimadzu, X-ray source is Cu). The optical absorption spectrum was obtained using a UV-VIS spectrophotometer 6800 JENWAY, Germany within the wavelength range of (300-1100) nm. For gas sensor measurements (sensitivity, response time ... etc) we depend upon the difference of resistance or the current through films when the surface of thin films dispose to (NO_2) at certain temperature.

Scanning Electron Microscope (SEM) type (Inspect S50) Japanese origin was used to study the surface of thin films (CeO_2-CuO). We used the system to know the sensitivity for different gases and they are the following parts. 1-Vacuum pumping (Rotary). 2-Connecting pipes. 3- Measurement for vacuum. 4- Chamber cylindrical stainless steel, diameter 30cm and 35cm high, and the chamber contain the following, A- Let for testing gas. B- Valve for entering the air after vacuum. C- Glass window. At the bottom or base of the chamber there is an electric heater as well as Thermocouple K-type it is used for controlling the operating temperature and for sensor electrodes. 5- DC-Power supply. 6- Resistance measurement. 7- Laptop for recording the difference of sensor current, when there is percent from gas which enrich the sensor by pipe to the inside of chamber to give the real sensitivity.

Results and discussion

a. Structural properties

The structure of the prepared copper oxide thin films were investigated by XRD, by observing the Table 1 and Fig. 1, which shows the results of X-ray diffraction, and compare these results with (ASTMs) (American Standard Testing of Materials) and the impact on silicon bases and thickness (175 nm). The results are fairly compatible all Prepared films are deposited on silicon

substrate at 200 °C, rules show that the films have Polycrystalline structure type monoclinic the tendency for these films is (111) as well as the emergence of a second peak less intensity ($11\bar{1}$), either the third peak was ($20\bar{2}$) which goes back to (CuO) when increase the percentage of cerium to (20, 30, 40, and 50) note increasing intensity of peaks due to copper oxide as well as the emergence of new peaks to cerium oxide with decreased in (FWHM), with variation in offset angles, It turns out that increasing the temperature of deposed structure had not changed the nature of the Crystal structure of the article but has increased the intensity of the peaks as in the Fig. 2 and 3. The result corresponds with that described by Motoyoshi, R et al. [19]. Grain size D was calculated using the X- ray diffraction results and it turns out that crystalline size increases with increasing doping [see Tables 2 and 3].

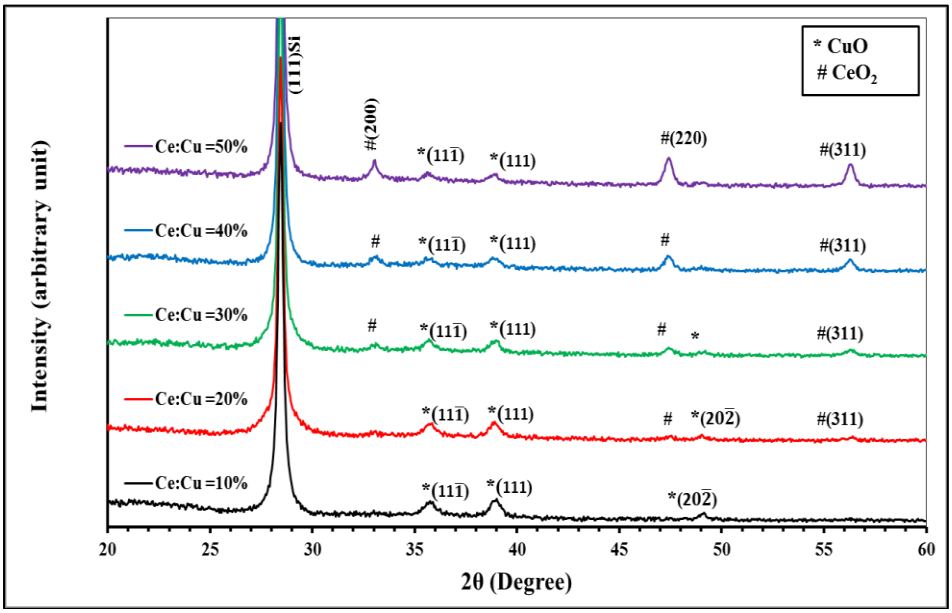

Fig.1: X-ray diffraction patterns of CuO :Ce thin films at 200 °C.

Table 1: Average crystallite size, d(hkl) and FWHM for Cerium - Cupric oxide thin films at 200 °C.

CeO_2 (%)	2θ (Deg.)	FWHM (Deg.)	d_{hkl} Exp.(Å)	G.S (nm)	hkl	d_{hkl} Std.(Å)	Phase	Card No.
10	35.7440	0.6340	2.5100	13.2	(11-1)	2.5108	CuO	96-900-8962
	38.9350	0.6000	2.3113	14.0	(111)	2.3118	CuO	96-900-8962
	49.0661	0.5600	1.8552	15.6	(20-2)	1.8553	CuO	96-900-8962
20	35.7316	0.6213	2.5108	13.4	(11-1)	2.5108	CuO	96-900-8962
	38.9226	0.5880	2.3120	14.3	(111)	2.3118	CuO	96-900-8962
	47.4390	0.5833	1.9149	14.9	(220)	1.9131	CeO_2	96-900-9009
	49.0537	0.5488	1.8556	15.9	(20-2)	1.8553	CuO	96-900-8962
	56.3090	0.5560	1.6325	16.2	(311)	1.6315	CeO_2	96-900-9009
30	33.0590	0.5068	2.7075	16.4	(200)	2.7055	CeO_2	96-900-8962
	35.7192	0.6089	2.5117	13.7	(11-1)	2.5108	CuO	96-900-8962
	38.9102	0.5762	2.3127	14.6	(111)	2.3118	CuO	96-900-8962
	47.4280	0.5308	1.9154	16.4	(220)	1.9131	CeO_2	96-900-9009
	49.0413	0.5378	1.8560	16.2	(20-2)	1.8553	CuO	96-900-8962
	56.2980	0.5060	1.6328	17.8	(311)	1.6315	CeO_2	96-900-9009
40	33.0480	0.4612	2.7083	18.0	(200)	2.7055	CeO_2	96-900-8962
	35.7068	0.5967	2.5125	14.0	(11-1)	2.5108	CuO	96-900-8962
	38.8978	0.5647	2.3134	14.9	(111)	2.3118	CuO	96-900-8962
	47.4170	0.4830	1.9158	18.0	(220)	1.9131	CeO_2	96-900-9009
	56.2870	0.4604	1.6331	19.6	(311)	1.6315	CeO_2	96-900-9009
50	33.0370	0.4197	2.7092	19.8	(200)	2.7055	CeO_2	96-900-8962
	35.6944	0.5848	2.5134	14.3	(11-1)	2.5108	CuO	96-900-8962
	38.8854	0.5534	2.3142	15.2	(111)	2.3118	CuO	96-900-8962
	47.4060	0.4396	1.9162	19.7	(220)	1.9131	CeO_2	96-900-9009
	56.2760	0.4190	1.6334	21.5	(311)	1.6315	CeO_2	96-900-9009

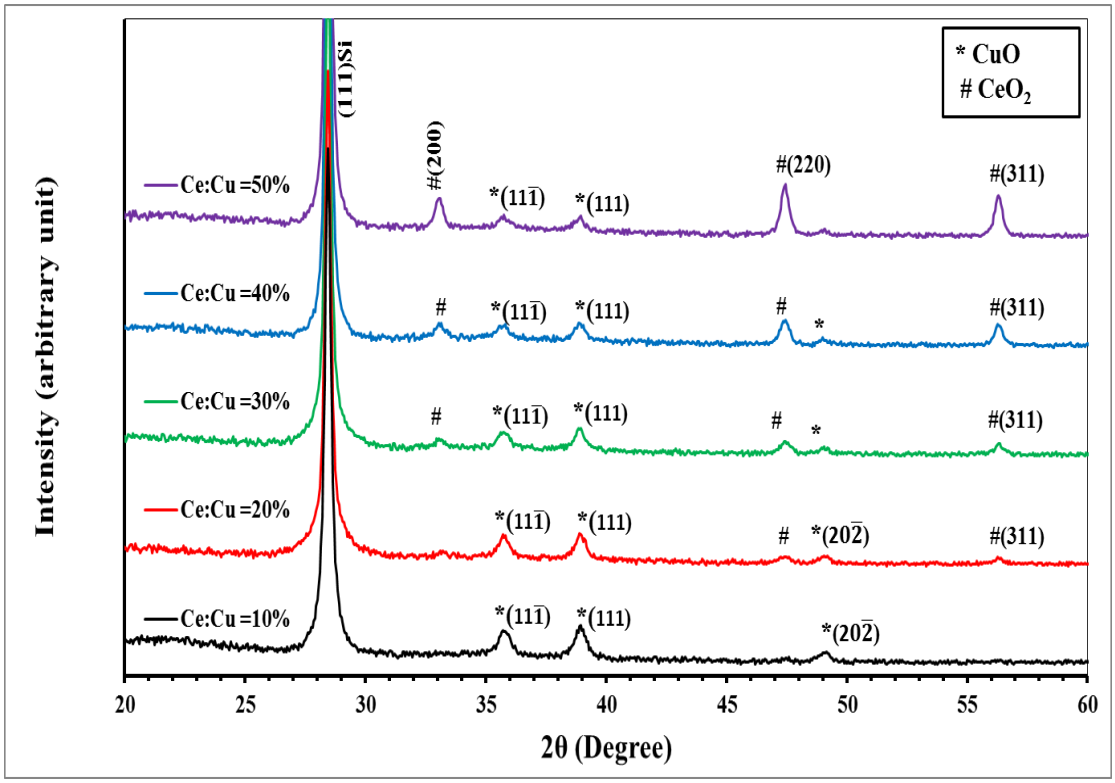

Fig.2: X-ray diffraction patterns of CuO: Ce thin films at 250 °C.

Table 2: Average crystallite size, d(hkl) and FWHM for Cerium - Cupric oxide thin films at 250 °C.

CeO_2 (%)	2θ (Deg.)	FWHM (Deg.)	d_{hkl} Exp.(Å)	G.S (nm)	hkl	d_{hkl} Std.(Å)	Phase	Card No.
10	35.7543	0.5706	2.5093	14.6	(11-1)	2.5108	CuO	96-900-8962
	38.9453	0.5400	2.3107	15.6	(111)	2.3118	CuO	96-900-8962
	49.0764	0.5040	1.8548	17.3	(20-2)	1.8553	CuO	96-900-8962
20	35.7419	0.5592	2.5101	14.9	(11-1)	2.5108	CuO	96-900-8962
	38.9329	0.5292	2.3114	15.9	(111)	2.3118	CuO	96-900-8962
	47.4603	0.5250	1.9141	16.5	(220)	1.9131	CeO_2	96-900-9009
	49.0640	0.4939	1.8552	17.7	(20-2)	1.8553	CuO	96-900-8962
	56.3303	0.5004	1.6319	18.0	(311)	1.6315	CeO_2	96-900-9009
30	33.0803	0.4561	2.7058	18.2	(200)	2.7055	CeO_2	96-900-8962
	35.7295	0.5480	2.5110	15.2	(11-1)	2.5108	CuO	96-900-8962
	38.9205	0.5186	2.3122	16.3	(111)	2.3118	CuO	96-900-8962
	47.4493	0.4777	1.9145	18.2	(220)	1.9131	CeO_2	96-900-9009
	49.0516	0.4840	1.8557	18.0	(20-2)	1.8553	CuO	96-900-8962
	56.3193	0.4554	1.6322	19.8	(311)	1.6315	CeO_2	96-900-9009
40	33.0693	0.4151	2.7067	20.0	(200)	2.7055	CeO_2	96-900-8962
	35.7171	0.5370	2.5118	15.5	(11-1)	2.5108	CuO	96-900-8962
	38.9081	0.5082	2.3129	16.6	(111)	2.3118	CuO	96-900-8962
	47.4383	0.4347	1.9150	20.0	(220)	1.9131	CeO_2	96-900-9009
	49.0392	0.4744	1.8561	18.4	(20-2)	1.8553	CuO	96-900-8962
	56.3083	0.4144	1.6325	21.8	(311)	1.6315	CeO_2	96-900-9009
50	33.0583	0.3777	2.7075	21.9	(200)	2.7055	CeO_2	96-900-8962
	35.7047	0.5263	2.5127	15.9	(11-1)	2.5108	CuO	96-900-8962
	38.8957	0.4981	2.3136	16.9	(111)	2.3118	CuO	96-900-8962
	47.4273	0.3956	1.9154	21.9	(220)	1.9131	CeO_2	96-900-9009
	56.2973	0.3771	1.6328	23.9	(311)	1.6315	CeO_2	96-900-9009

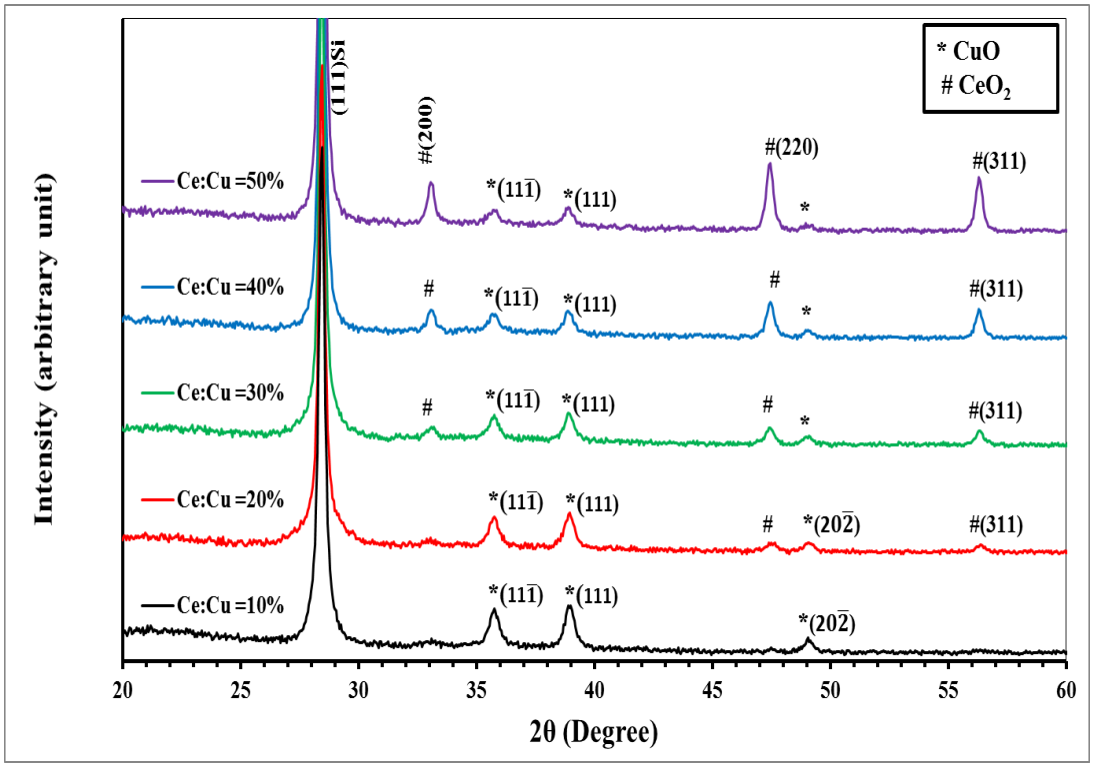

Fig .3: X-ray diffraction patterns of CuO: Ce thin films at 300 °C.

Table 3: Average crystallite size, d(hkl) and FWHM for Cerium - Cupric oxide thin films at 300 °C.

CeO_2 (%)	2θ (Deg.)	FWHM (Deg.)	d_{hkl} Exp.(Å)	G.S (nm)	hkl	d_{hkl} Std.(Å)	Phase	Card No.
10	35.7646	0.5135	2.5086	16.3	(11-1)	2.5108	CuO	96-900-8962
	38.9556	0.4860	2.3101	17.3	(111)	2.3118	CuO	96-900-8962
	49.0867	0.4536	1.8544	19.3	(20-2)	1.8553	CuO	96-900-8962
20	35.7522	0.5033	2.5095	16.6	(11-1)	2.5108	CuO	96-900-8962
	38.9432	0.4763	2.3109	17.7	(111)	2.3118	CuO	96-900-8962
	47.4706	0.4725	1.9137	18.4	(220)	1.9131	CeO_2	96-900-9009
	49.0743	0.4445	1.8549	19.7	(20-2)	1.8553	CuO	96-900-8962
	56.3406	0.4504	1.6317	20.0	(311)	1.6315	CeO_2	96-900-9009
30	33.0906	0.4105	2.7050	20.2	(200)	2.7055	CeO_2	96-900-8962
	35.7398	0.4932	2.5103	16.9	(11-1)	2.5108	CuO	96-900-8962
	38.9308	0.4668	2.3116	18.1	(111)	2.3118	CuO	96-900-8962
	47.4596	0.4300	1.9142	20.2	(220)	1.9131	CeO_2	96-900-9009
	49.0619	0.4356	1.8553	20.1	(20-2)	1.8553	CuO	96-900-8962
	56.3296	0.4098	1.6320	22.0	(311)	1.6315	CeO_2	96-900-9009
40	33.0796	0.3736	2.7058	22.2	(200)	2.7055	CeO_2	96-900-8962
	35.7274	0.4833	2.5111	17.3	(11-1)	2.5108	CuO	96-900-8962
	38.9184	0.4574	2.3123	18.4	(111)	2.3118	CuO	96-900-8962
	47.4486	0.3913	1.9146	22.2	(220)	1.9131	CeO_2	96-900-9009
	49.0495	0.4269	1.8558	20.5	(20-2)	1.8553	CuO	96-900-8962
	56.3186	0.3729	1.6323	24.2	(311)	1.6315	CeO_2	96-900-9009
50	33.0686	0.3399	2.7067	24.4	(200)	2.7055	CeO_2	96-900-8962
	35.7150	0.4737	2.5120	17.6	(11-1)	2.5108	CuO	96-900-8962
	38.9060	0.4483	2.3130	18.8	(111)	2.3118	CuO	96-900-8962
	47.4376	0.3560	1.9150	24.4	(220)	1.9131	CeO_2	96-900-9009
	49.0371	0.4184	1.8562	20.9	(20-2)	1.8553	CuO	96-900-8962
	56.3076	0.3394	1.6325	26.6	(311)	1.6315	CeO_2	96-900-9009

The scanning electron microscopy (SEM) was used to study the surface topography of (CuO:Ce %) on a glass base at a temperature of (200 °C) and with ratio 50%. The thickness of the membrane shows a clear smoothness. This indicates that the granules that have grown on the surface of the membrane have almost the same form and size, and the thickness of the films

is about 50%. As the addition of cerium, the surface topography of the film increases in surface roughness (RMS). Roughness is associated with the sensitivity of the surface of the film as it increases the interaction with the gas [20]. The granules appear in clusters which formed by the surface of the film and the boundaries of the particles appear intersecting between them. Increasing the particle size to some degree in addition can reduce the effect of these defects. Fig. 4 shows the elements involved in the thin film composition of CuO: Ce and strongly enlarge (2 um).

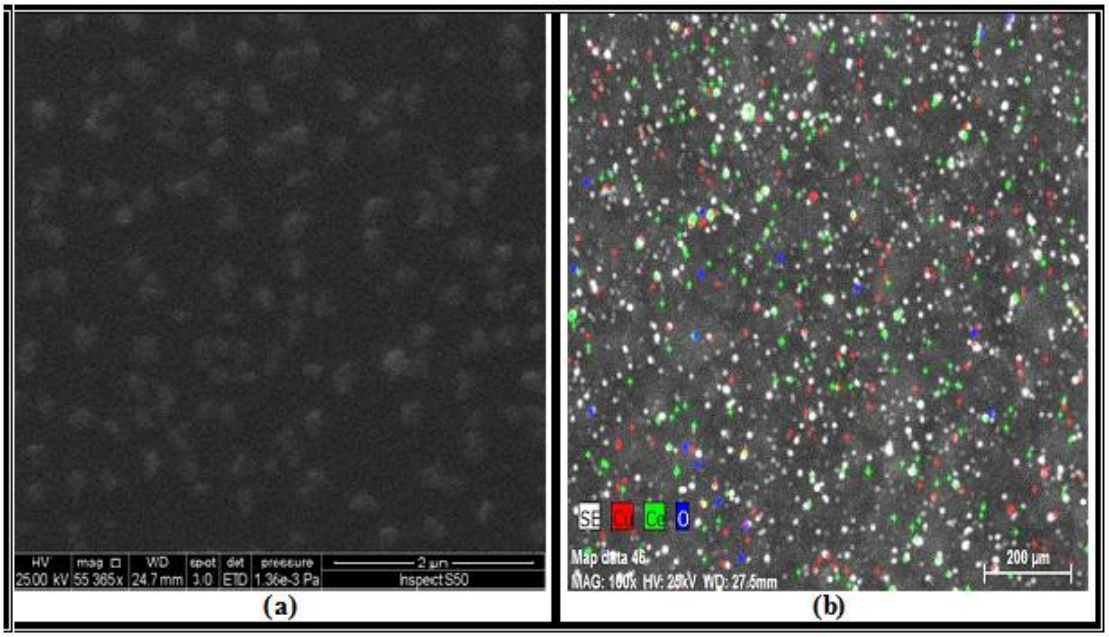

Fig. 4: SEM images of the film (CuO: Ce): (a) after the addition of Ce 50% (b) Elements involved in film formation.

b. Optical properties

The application of the relationship(1) of the optical absorption factor (α) was found by absorption of the spectrum (A) of the prepared films where it was found that the coefficient of absorption has the values of all films (CuO:Ce%) larger than the rates (10^4 cm^{-1}) Visible spectrum. This indicates that all prepared thin films have a direct energy gap, and the value of (r) in the relationship (2) is equal to (1/2). The relationship between the absorption coefficient (α) and the wavelength (λ) of the membranes (CuO: Ce%) at (Ce = 0.10, 0.20, 0.30, 0.40, 0.50) and at the base temperature (200 ˚C) as in (Fig. 5a) indicating that the absorption edge, which represents the lowest value of the absorption factor, is at the wavelength (λc) by linear extension of the low values of the absorption coefficient. When (Ce = 10%), the thin film (CuO: Ce%) has an (λc) equal to (840nm). When the ratio of cerium (Ce = 50%) is the wavelength of the film to the limits of (600 nm) of the visible spectrum, during the observation of the shape of the rest of the films, there is a small shift in the edge of absorption towards high wavelength, (CuO) in the prepared films due to the fact that CuO films have a direct power gap less than CeO_2 and have a high absorption factor. "The higher absorption coefficient indicates that transitions directly from the valence pack to a coupling package called transitions (band to band) because of the basic absorption process and these results correspond to what the researchers say." [21], either in the

case of increasing the temperature of rules to sedimentation (250, 300˚C) note increased absorption coefficient with each ratio of cerium and this is shown in Figs. 5b and 5c.

$$\alpha=2.303(A/t) \quad (1)$$

α: Absorption coefficient (cm^{-1})

$$\alpha h\upsilon = A_o\left(h\upsilon - E_g\right)^r \quad (2)$$

h: blank constant

A_o : Constant determined by the nature of the transition.

r: (1/2, 3/2، 2،3) the exponential coefficient determines the nature of the transition.

υ : Frequency of beam.

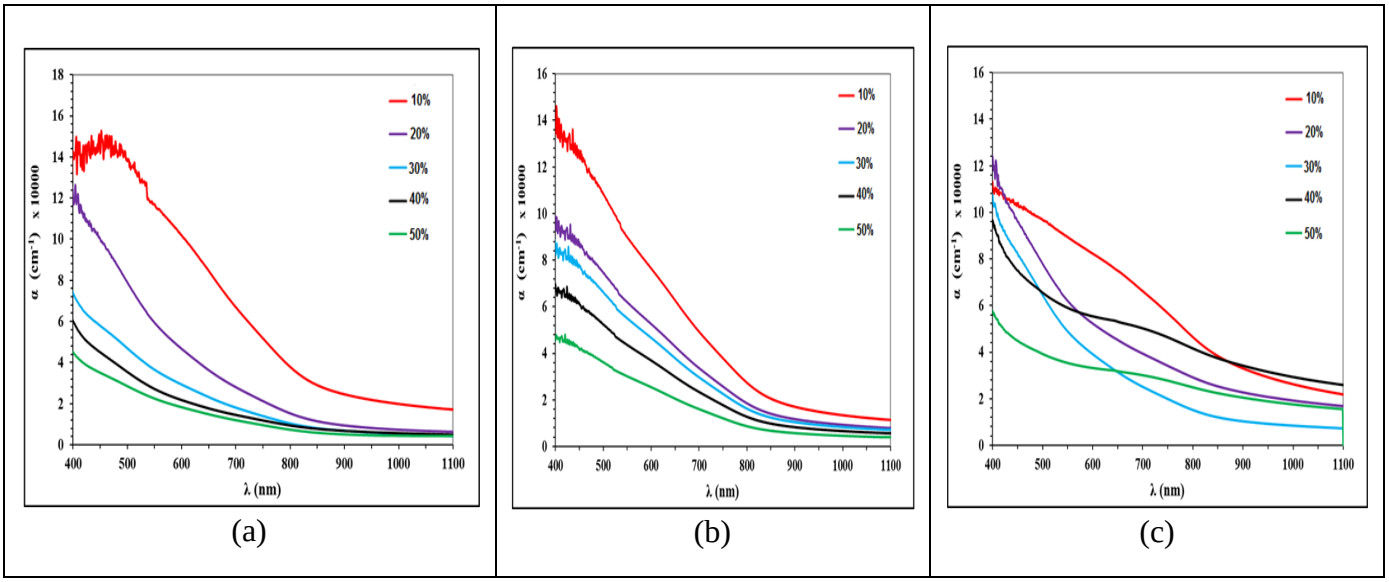

Fig.5: (a) Change absorption coefficient α with the λ at (200 ˚C). (b) Absorption coefficient α with the λ at (250 ˚C). (c) Absorption coefficient α with the λ at (300 ˚C).

The optical energy gap values were calculated for films prepared for Allowable direct transition for all copper oxide films [22, 23] by using the relation (3).

$$(\alpha h\nu)^2= \beta(h\upsilon - E_g) \quad (3)$$

where α is the absorption coefficient, β is a constant, Eg is the optical energy gap, υ is the incident photon frequency, and h is the Planck constant.

The relationship between $(\alpha h\nu)^2$ as a function of photon energy (hν) and that tangent line the straight part of the curve represents the value of the optical energy gap of the allowed direct transition, most researchers depend on this way calculate the energy gap (Balamurugan et al.) [24], as well as researchers (M. S. Dresselhaus et al.) [25], for Cupric oxide films with Ce (10, 20, 30, 40, 50 %), Energy gap values gradually increased with increasing proportions of cerium. This means that the addition leads to the displacement of the fundamental absorption edge toward high energies when the degree of the base 200 ^oC. When the temperature increases at 250, 300 ^oC, we observe a small red shift of the energy gap values towards the lower values as the temperature of the precipitation rules increases as in Fig.6. Table 4 shows the energy gap for all films prepared values.

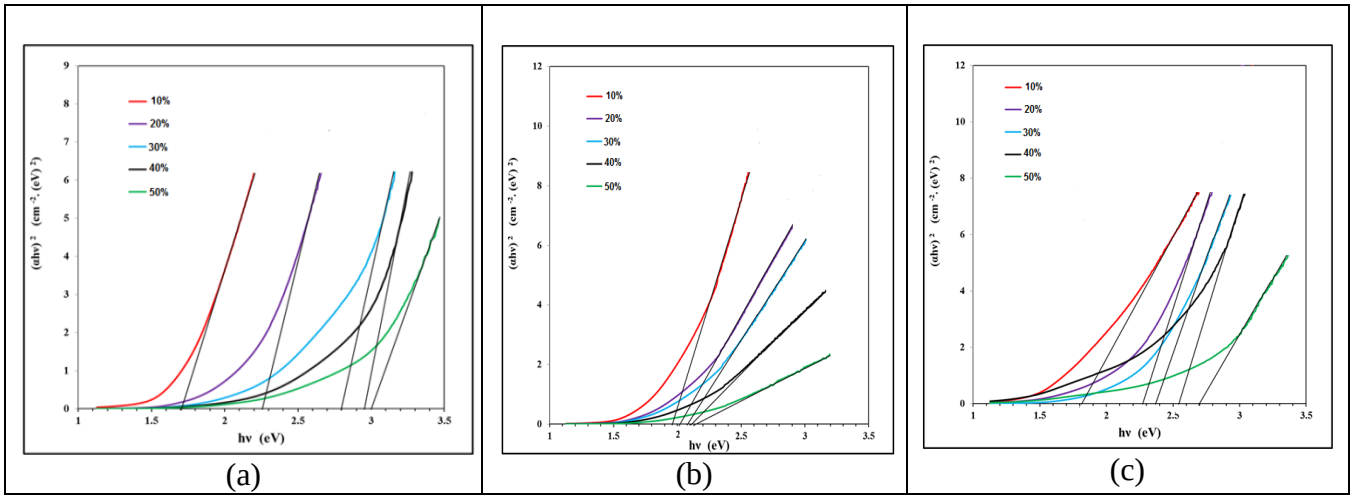

Fig. 6: Band gap for CuO-CeO_2 films at different temperature a) 200 ^oC, b) 250 ^oC and c) 300 ^oC.

Table 4: Band gap energies calculated with Tauc method.

Ce%	Eg (eV) at 200 ^oC	Eg (eV) at 250 ^oC	Eg (eV) at 300 ^oC
10%	1.70	1.95	1.80
20%	2.25	2.05	2.20
30%	2.80	2.08	2.37
40%	2.95	2.12	2.55
50%	3.00	2.15	2.70

Sensitive properties

A-temperature effect on gas sensor

The work of the gas sensor depends mainly on the temperature at the base of the sensor it is an important factor in the process of interaction of the surface of the oxide or the surface of the films with the gas and therefore it is necessary to know the operating temperature to identify the response of the sensor and to know the greatest value of the response and also know whether the sensor works to room temperature or not? because it is an important characteristic of a good sensor, therefore, in our study we take into account the range of different temperatures, starting from room temperature (25 °C) to (300 °C), and the nitrogen dioxide (NO_2) by 3%, shown in Fig.7a sensitivity change with temperature sensors (CuO: Ce%) at the ratio of cerium (Ce=10%) where it was found that the sensor work at room temperature and this is a good idea to work the sensor with this degree of heat [26-28], although the sensitivity was low, where the sensitivity is equal to the value of (1.8%), this value began to increase as the operating temperature increase, either the greatest value (26.79%) at the operating temperature (300 °C).

In Fig.7b we observe a change in the response time and recovery time with temperature; we note that the lowest value is 18,81 sec, respectively. This shows the rapid response of the sensor (CuO:Ce%). Fig.8a shows the sensitivity as a function of the temperature at the rate (Ce = 50%) as it is clear that the sensitivity increases with the increase of the addition of cerium, Fig. 8b shows the response time, and the time of recovery change with temperature change operating as we notice its low values with increased percentages added.

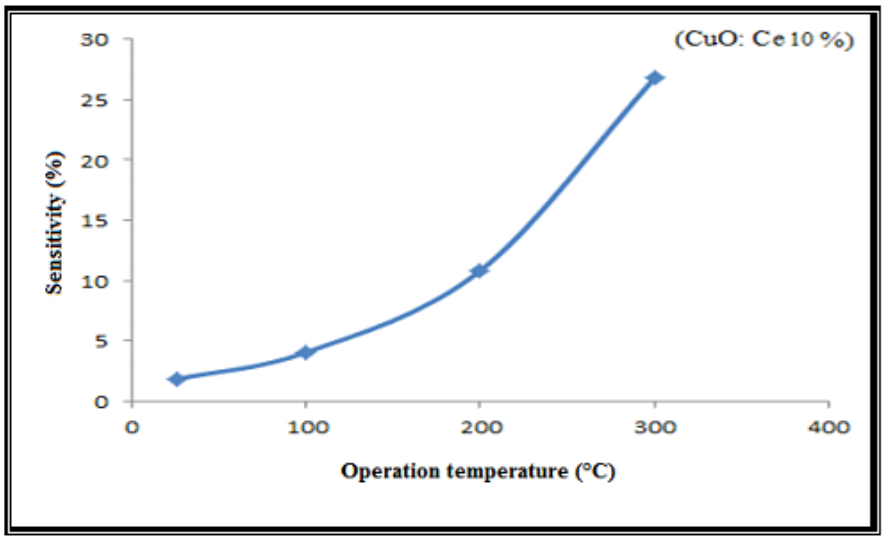

Fig.7a: Sensitivity of films (CuO: Ce%) with operating temperature at (Ce 10%) and NO_2= 3 %.

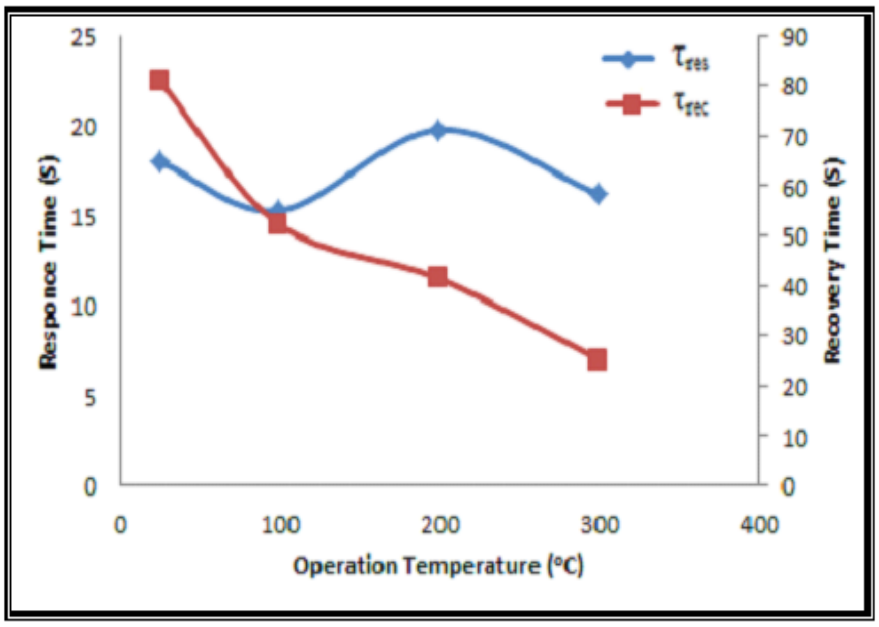

Fig.7b: Change the response time and recovery time of the films (CuO:Ce%) with the operating temperature at the ratio (Ce = 10%) and NO_2= 3 %.

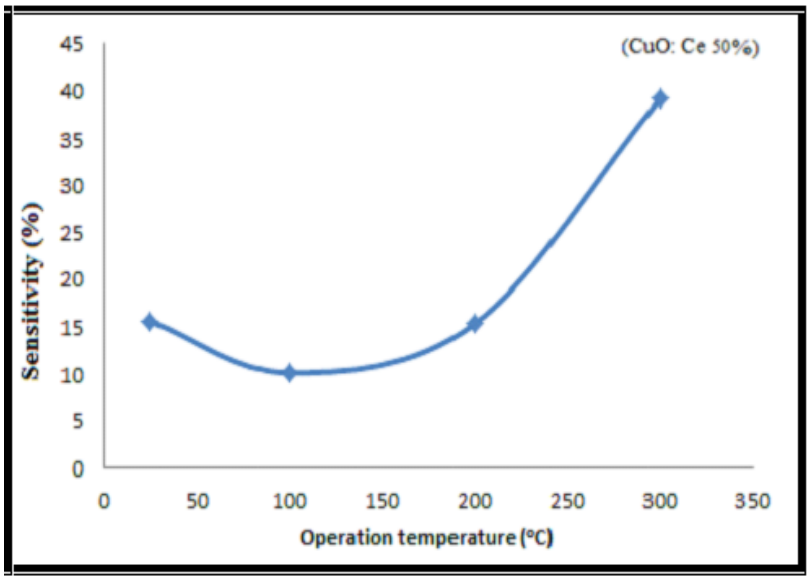

Fig. 8a: Sensitivity of films (CuO: Ce%) with operating temperature at (Ce 50%) and NO_2= 3 %.

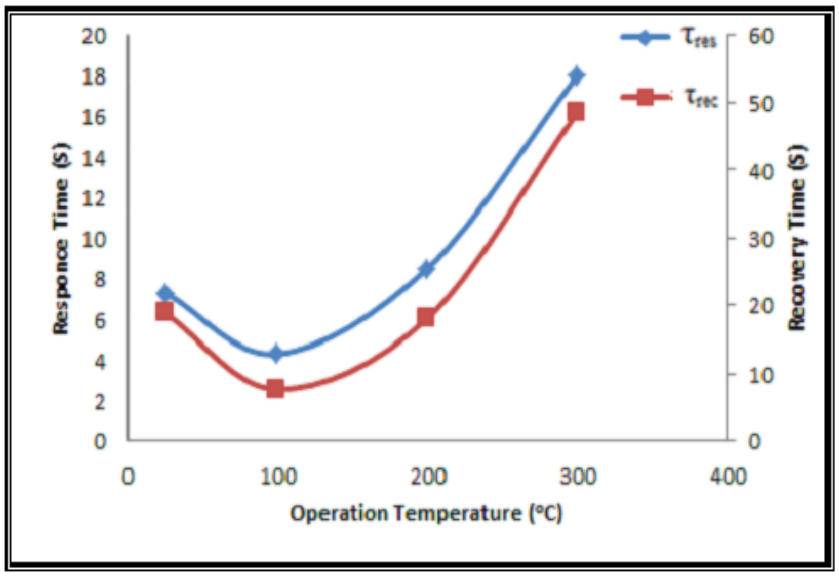

Fig.8b: Change the response time and recovery time of the films (CuO:Ce%) with the operating temperature at the ratio (Ce = 50%) and NO_2= 3 %.

Conclusions

All the films have Polycrystalline structure type Monoclinic the tendency has been for these films is (111) at temperatures substrate (200, 250 and 300 ^{o}C), Adding cerium did not change the nature of the crystal structure, adding led to an increase in crystal size (***D***) with decreasing width mid-intensity (***FWHM***) as show by the X- ray results, X-ray results show that granular structures are within the structure of nanoparticles. The surface topography film increase in roughness led to increases the root mean square (RMS). Roughness is associated with the surface sensitivity of the film as it increases the interaction with the gas and this is evidenced by the results of SEM. Increased films permeability and decreased absorbance with increased Ce % ratios, and increased energy gap with increased cerium ratios. The results showed that films (CuO:Ce%) by the pyrolysis method of chemical

spray prepared have the characteristics of the sensitivity of the NO_2 good gas.

References

[1] B.J. Chens, X.W. Sun, B.K. Tay, Mater. Sci. Eng. B., 106 (2004) 300-304.
[2] Chengxiang Wang, Longwei Yin, Luyuan Zhang, Dong Xiang, RuiGao, Sensors, 10 (2010) 2088-2106.
[3] X.P. Gao, J.L. Bao, G.L. Pan, H.Y. Zhu, P.X. Huang, F. Wu, D.Y. Song, J. Phys. Chem, 108 (2004) 5547-5551.
[4] H.M. Xiao, S.Y. Fu, L.P. Zhu, Y.Q. Li, G. Yang, Eur, J. Inorg. Chem, 14 (2007) 1966-1971.
[5] H. Fan, L. Yang, W. Hua, X. Wu, Z. Wu, S. Xie, B. Zou, Nanotechnology Nanotechnology, 15 (2008) 37-42.
[6] C.T. Hsieh, J.M. Chen, H.H. Lin, H.C. Shih, Applied Physics Letters, 83, 16 (2003) 3383-3385.
[7] P.O. Larsson, A. Andersson, R.L. Wallengerg, B. Svensson, J. Catal, 163 (1996) 279-293.
[8] W. Chae, J. Ho Yoon, H. Yu, D. Jang, Y. Kim, J. Phys. Chem., 108, 31 (2004) 11509-11513.
[9] Y. L. Liu, Y. C. Liu, R. Mu, H. Yang, C. L. Shao, J. Y. Zhang, Y. M. Lu, D. Z. Shen, X. W. Fan, Semicond. Sci. and Tech., 20 (2005) 44-49.
[10] Y. C. Zhou and J. A. Switzer, Mater. Res. Innovat., 2 (1998) 22-27.
[11] T. Maruyama, Jpn. J. Appl. Phys., 37 (2000) 4099-4102.
[12] V. Figueiredo, E. Elangovan, G. Gonçalves, P. Barquinha, L. Pereira, N. Franco, E. Alves, R. Martins, and E. Fortunato, Applied Surface Science, 254 (2008) 3949-3954.
[13] R. Kita, K. Kawaguchi, T. Hase, T. Koga, R. Itti, T. Morishita, J. Mater. Res., 9 (1994) 1280-1283.
[14] Xinxin Ma, Gang Wang, Ken Yukimura, Mingren Sun, Surface and Coatings Technology, 201 (2007) 6712- 6714.
[15] F. Drobny and D. Pulfrey, Thin Solid Films, 502, (1/2) (2006) 205-211.
[16] F. Bayansal, B. Sahin, M. Yuksel, H.A. Cetinkara J. Materials Letters, 98 Provider: Elsevier (2013) 197-200.
[17] M. Izaki, J. Thin Solid Films 520, Provider: Elsevier (2012) 2434- 2437.
[18] Z. H. Gans, G. Q. Yu, B. K. Tay, C. M. Tan, Z. W. Zhao, Y. Q. Fu, J. Appl. Phys., 37 (2004) 81-85.
[19] R. Motoyoshi, T. Oku, H. Kidowaki, A. Suzuki, K. Kikuchi, S. Kikuchi, B. Jeyadevan, J. of The Ceramic Society of Japan 118, (1383) (2010) 1021-1023.
[20] Arijit Chowdhuri, Vinay Gupta K. Sreenivas, Rev. Adv. Mater. Sci., 4 (2003) 75-78.
[21] Y. J. Tian, S. Linzen, F. Schmidl, A. Matthes, Thin Solid Films, 338 (2003) 224-230.
[22] C. Ray. Sekhar. J. of Physics. Solar Energy Materials and Solar Cells, 68 (2001) 307-312.
[23] A.A. Ogwu, E. Bouquerel, O. Ademosu, S. Moh, E. Crossan, F. Placido, Electronic Engineering and Physics Division, Acta. Materialia, 53 (2005) 5151-5159.
[24] E. Mohandas, G. Balakrishnan, S. Tripura Sundari. Elsevier, Science Direct. Thin Solid Films, 10 Dec, (2010) 520-526.
[25] M. S. Dresselhaus, "Optical Properties of Solids" Part II, 1998.
[26] G.N. Papadimitropoulos, N. Vourdas, E. Vamvakas, D. Davazoglou, Thin Solid Films, 515 (2006) 2428-2432.
[27] X. Zhou, Q. Cao, H. Huang, P. Yang, Y. Hu, Mater. Sci. Eng. B, 99 (2003) 44-47.
[28] A. Chowdhuri, V. Gupta, K. Sreenivas, Sens. Actuators B, 93 (2003) 572-579.